

Electronic Supplementary Information

Pyrolysis of a metal-organic framework followed by *in situ* X-ray absorption spectroscopy, powder diffraction and pair distribution function analysis

Mads Folkjær,^{a,b} Lars F. Lundegaard,^c Henrik S. Jeppesen,^a Melissa J. Marks,^a Mathias S. Hvid,^a Sara Frank,^b Giannantonio Cibin,^d and Nina Lock^{e*}

^aInterdisciplinary Nanoscience Center (iNANO), Aarhus University, Gustav Wieds Vej 14, DK-8000 Aarhus C, Denmark

^bDepartment of Biological and Chemical Engineering, Aarhus University, Åbogade 40, DK-8200 Aarhus N, Denmark

^cHaldor Topsøe A/S, Haldor Topsøes Allé 1, DK-2800 Kgs. Lyngby, Denmark

^dDiamond Light Source Ltd., Harwell Science and Innovation Campus, Didcot, OX11 0DE, UK

^eCarbon Dioxide Activation Center (CADIAC), Department of Biological and Chemical Engineering and iNANO, Aarhus University, Åbogade 40, DK-8200 Aarhus N, Denmark

*Corresponding author: nlock@bce.au.dk

1. Scanning electron microscopy (SEM)	p. 2
2. Elemental analysis of pyrolyzed sample	p. 2
3. Heating profiles for all experiments	p. 3
4. X-ray absorption spectroscopy (XAS)	p. 4
4.1. Setup	p. 4
4.2. XANES linear combination analysis (LCA)	p. 5
4.3. Extended X-ray Absorption Fine Structure (EXAFS)	p. 7
5. Powder X-ray diffraction (PXRD)	p. 8
6. X-ray total scattering and pair distribution function (PDF) analysis	p. 17
6.1. Setup	p. 17
6.2. 2 °C/min pyrolysis experiment	p. 18
6.3. 5 °C/min pyrolysis experiment	p. 24
6.4. Rapid heating pyrolysis experiment	p. 26
7. PXRD and PDF scale factors	p. 28

1. Scanning electron microscopy (SEM)

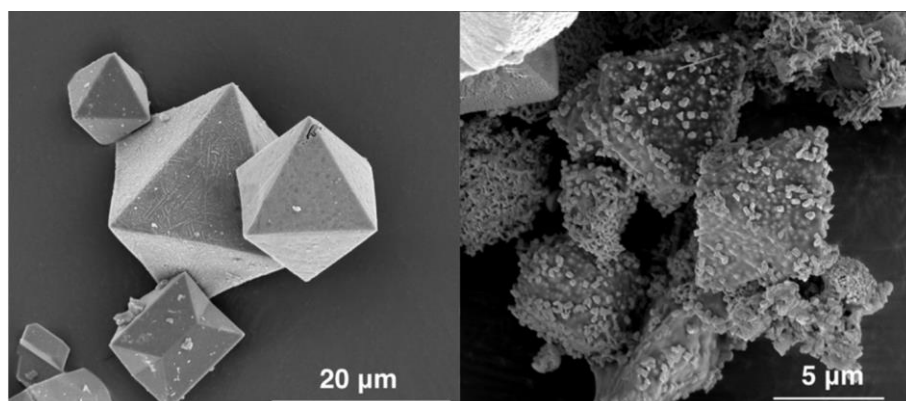


Fig. S1. Scanning electron micrographs of pristine (left) and pyrolyzed (right) HKUST-1 from 2 °C/min pyrolysis total scattering experiment.

2. Elemental analysis of pyrolyzed sample

HKUST-1 powder was pyrolyzed to 500 °C in a Nabertherm tube furnace with a heating ramp of 2 °C/min and a 100 mL/min N₂ flow. The sample was investigated by elemental (CHNS) analysis.

Table S1. CHNS analysis on HKUST-1 pyrolyzed in a tube furnace (500 °C, 2 °C/min, 100 mL/min N₂)

	Weight percentage
C	31.6(1)
H	0.87(3)
N	0.297(6)
S	0.07(1)

With the assumption that the remainder is Cu (i.e. assuming the O content to be negligible), the pyrolysis product consists of Cu (67.2 wt%), C (31.6 wt%), and H (0.9 wt%). The weight percentages are converted into atomic percentages to obtain the chemical formula CuC_{2.49}H_{0.81}, i.e., the carbon matrix in which the metallic copper is distributed has a C:H ratio of 3.06:1. The N and S contents are negligible.

3. Heating profiles of all experiments

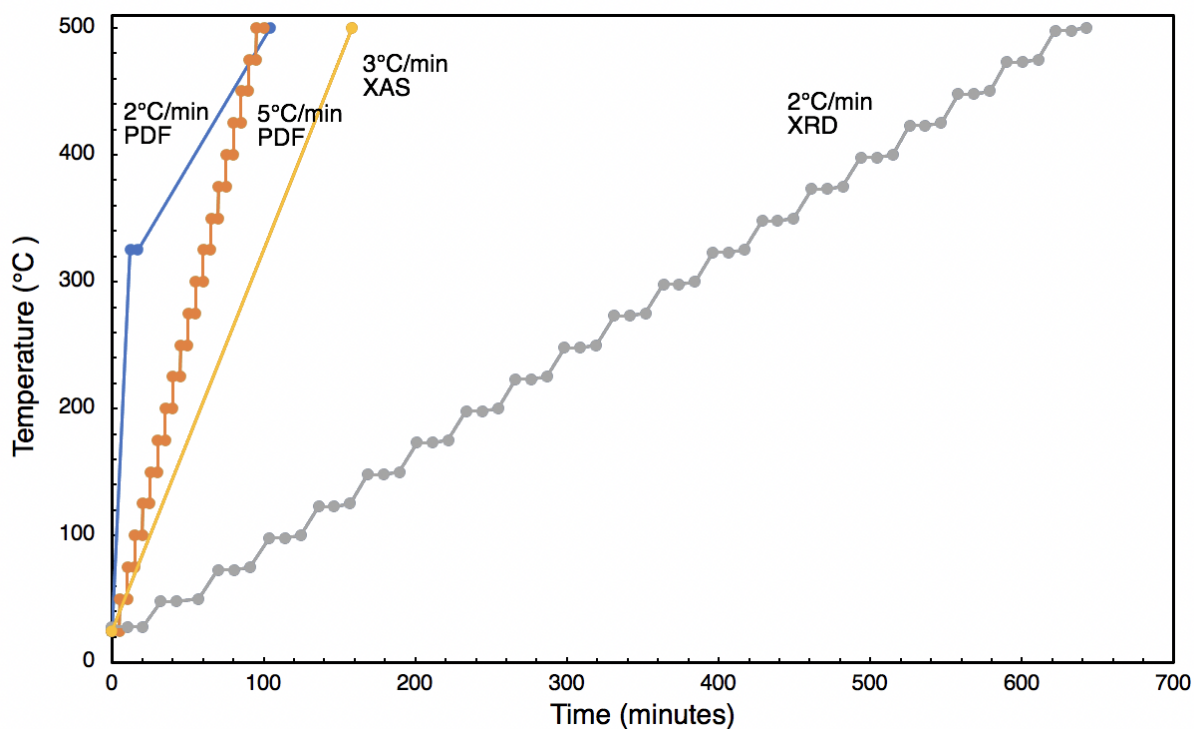


Fig. S2. Heating profiles used for the different *in situ* experiments. The 5 °C/min PDF and 2 °C/min PXRd heating were obtained by a stepwise profile (on average the PXRd heating ramp is 0.72 °C/min), while the 2 °C/min PDF and 3 °C/min XAS were both a continuous type of heating. Due to time constraints, the 2 °C/min PDF consisted of an initial 25 °C/min ramp until 325 °C was reached, after which the desired 2 °C/min heating ramp was employed. The difference in the 2 °C/min PDF and 3 °C/min XAS experiments were an unfortunate mishap due to overlap of the two beamtimes, as these experiments were both meant to be conducted with the same heating ramp.

4. X-ray absorption spectroscopy

4.1 Setup

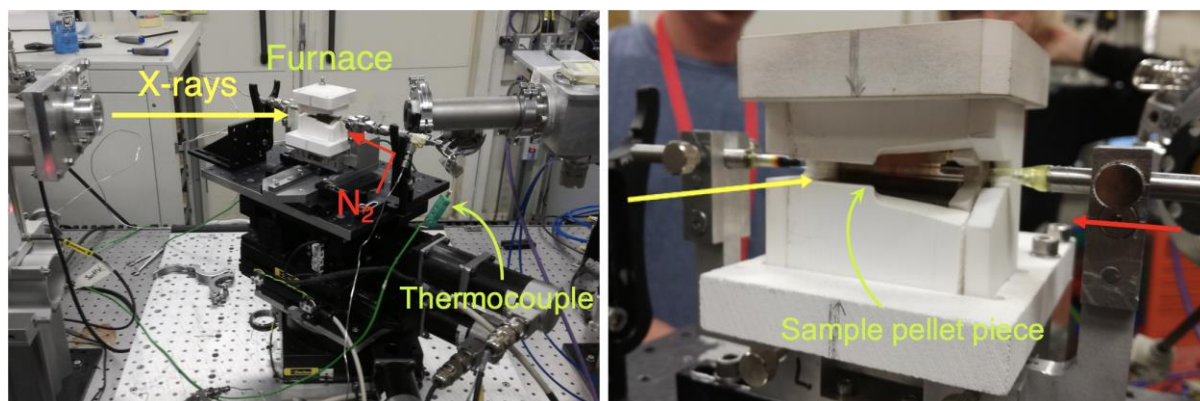


Fig. S3. *In situ* heating furnace available at the Diamond Light Source. A pellet with HKUST-1 diluted by boron nitride was inserted into a 3 mm quartz capillary, which was connected to Swagelok tubing, and the sample was purged by a nitrogen flow of 100 mL/min. The sample was heated from room temperature (RT) to 500 °C by indirect resistance heating with a heating ramp of 3 °C/min. A thermocouple was inserted into the tube to control the temperature. The furnace is designed to allow both fluorescence and transmission of X-rays but only the transmitted signal is used in this study.

4.2 XANES linear combination analysis (LCA)

Table S2. LCA fitting results. The temperature, *R*-factor, reduced chi-square (χ_v^2), chi-square (χ^2), weight fractions of HKUST-1, copper(I) oxide, and metallic copper and their respective uncertainties are reported. The spectra used for the analysis are collected over approx. 3 minutes (2 summed spectra) for the temperature range 264.5-367 °C, otherwise over approx. 15 minutes (10 summed spectra), where each spectrum was collected within approx. 90 seconds. The phase fractions were obtained from the LCA analysis as atomic percentages of copper. These data were converted into weight fractions to allow comparison with results from the PXRD and PDF analyses. In the data conversion it is assumed that the chemical composition of HKUST-1 is unchanged as $\text{Cu}_3(\text{btc})_2$.

Temp. (°C)	<i>R</i> -factor	χ_v^2	χ^2	HKUST-1 (wt%)	error (wt%)	Cu_2O (wt%)	error (wt%)	Cu (wt%)	error (wt%)
68	0.000159	0.000037	0.006190	100.00	0.00	0.00	0.00	0.00	0.00
109.5	0.000304	0.000069	0.011660	100.00	0.00	0.00	0.00	0.00	0.00
148	0.000433	0.000098	0.016520	100.00	0.00	0.00	0.00	0.00	0.00
190	0.000393	0.000089	0.014890	97.99	0.52	0.39	0.34	1.62	4.25
213	0.000592	0.000134	0.022310	96.58	0.65	1.78	0.55	1.65	0.43
264.5	0.000989	0.000218	0.036360	93.41	0.86	3.64	0.98	2.95	0.58
288	0.001542	0.000332	0.055400	90.49	1.13	5.43	0.75	4.08	4.11
289.5	0.002119	0.000448	0.074750	87.89	1.35	8.23	0.93	3.87	4.24
299	0.002394	0.000500	0.083480	84.36	1.45	10.30	1.68	5.34	1.01
305	0.003049	0.000619	0.103400	78.64	1.69	13.13	1.35	8.23	4.56
310.5	0.004882	0.000975	0.162870	56.28	5.17	33.00	2.58	10.72	2.36
318	0.008498	0.001602	0.267590	5.45	0.44	68.79	7.79	25.76	4.53
329	0.013938	0.002535	0.423330	0.00	0.00	77.06	6.44	22.94	4.50
336	0.010463	0.001798	0.302000	0.00	0.00	65.30	6.50	34.70	3.58
345.5	0.005872	0.000966	0.162300	0.00	0.00	46.52	4.11	53.48	2.68
355.5	0.007774	0.001246	0.209350	0.00	0.00	0.00	0.00	100.00	0.00
357.5	0.007913	0.001241	0.208550	0.00	0.00	0.00	0.00	100.00	0.00
367	0.007424	0.001171	0.196740	0.00	0.00	0.00	0.00	100.00	0.00
392.5	0.007293	0.001144	0.192240	0.00	0.00	0.00	0.00	100.00	0.00
431.5	0.006821	0.001065	0.178890	0.00	0.00	0.00	0.00	100.00	0.00
468.5	0.007604	0.001185	0.199060	0.00	0.00	0.00	0.00	100.00	0.00
500	0.007955	0.001236	0.207570	0.00	0.00	0.00	0.00	100.00	0.00

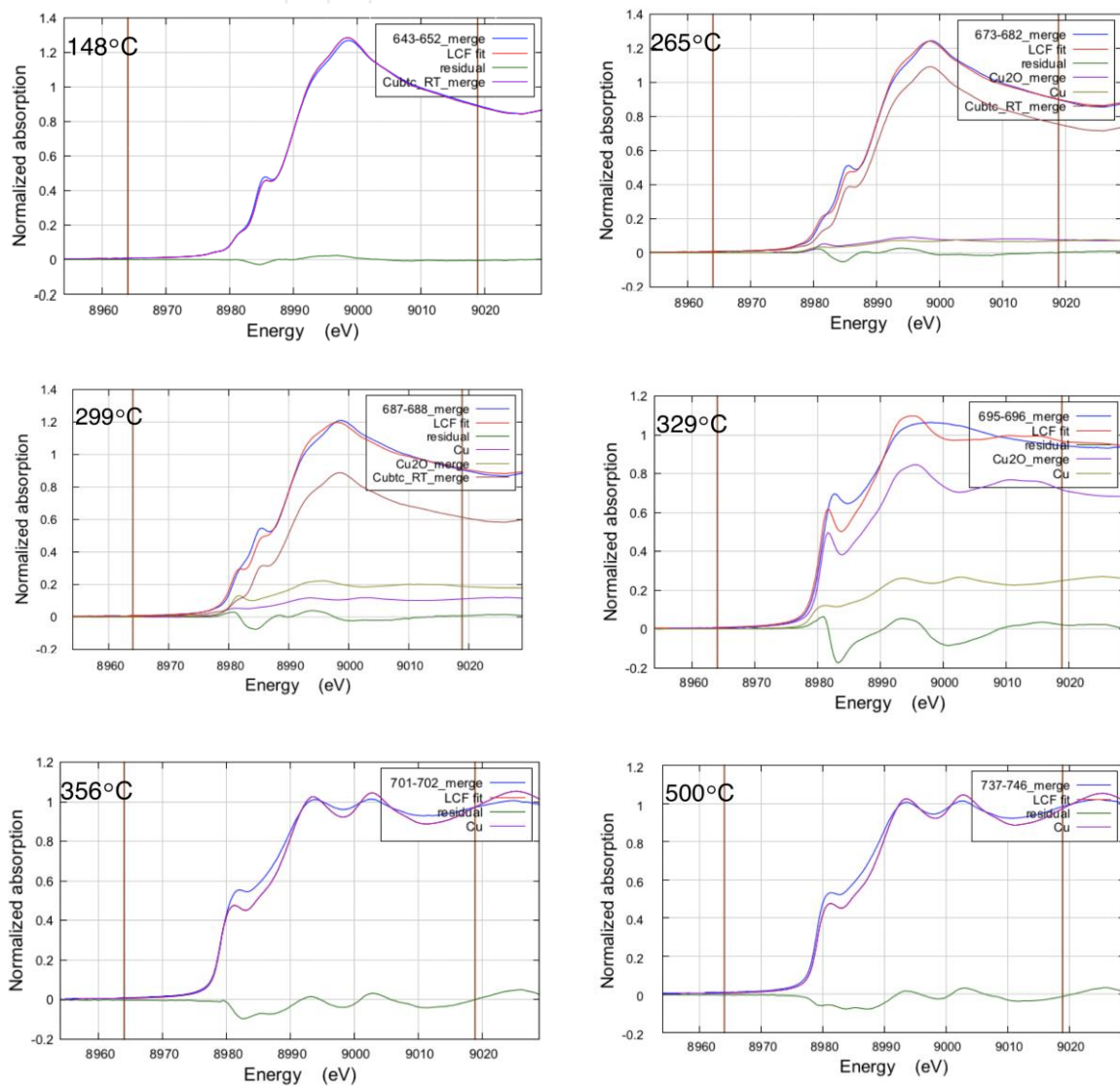


Fig. S4. Selected LCA fits. The blue line is the measured spectrum, the red line is the LCA fit, while the green line is the fit residual. Remaining lines are the HKUST-1, copper(I) oxide, and metallic copper linear combination components. The brown vertical lines show the fitting range. The temperature is displayed in top left of the plots.

4.3 Extended X-ray Absorption Fine Structure (EXAFS)

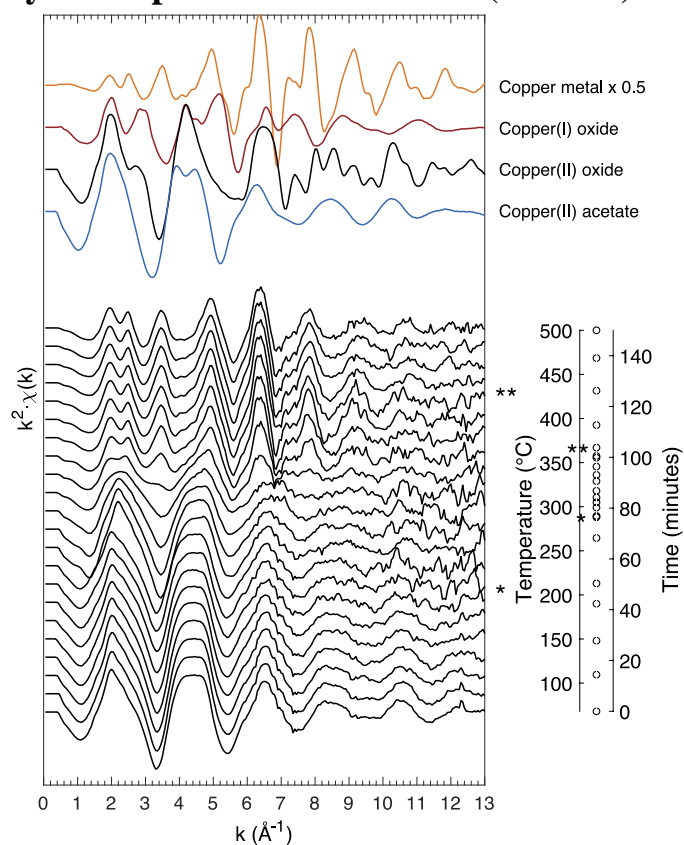


Fig. S5. EXAFS spectra of *in situ* pyrolysis. Four relevant standards are shown in top of the plot: Copper metal (yellow, scaled by 50%), copper(I) oxide (red), copper(II) oxide (black), and copper(II) acetate (blue). A combined temperature/time axis is shown on the right of the figure. As the plotted EXAFS spectra are not equidistant in temperature/time, asterisks (* and ***) are used to indicate the start and end of a narrower temperature interval where most of the chemistry occurs, i.e. 288-367 $^{\circ}\text{C}$. Open circles (o) indicate temperatures at which data are shown.

5. Powder X-ray diffraction (PXRD)

Table S3. Results from sequential Rietveld refinement of PXRD data. Reported are the time in hours (heating profile displayed in Fig. S2), the temperature in degrees Celsius, R_{wp} in percentage, the phase fractions in weight percentage, the crystallite size (D) in Angstrom, the scale factor, and cubic unit cell parameter (a) in Angstrom. The evaporation of water in HKUST-1 upon heating was taken into account by refining the occupancies of the pore (Ow1) and ligand (O1) water oxygen atoms. A peak at $\sim 23^\circ$ (2θ) is introduced into the refinements as a separate ‘peak’ phase. We have not been able to identify this phase, but as it disappears before the decomposition of HKUST-1 we do not believe it influences the results. The HKUST-1 phase was removed from the refinements when no peaks from this phase could be visually detected. One size parameter was refined for each of the three crystalline phases, *i.e.* HKUST-1, Cu₂O and Cu. The particle sizes were constrained to have minimum values of 100 Å for Cu₂O, 200 Å for Cu, and 800 Å for HKUST-1 to avoid correlation with background parameters in datasets with low content of these phases. The minimum values were estimated by visual inspection of the Rietveld fit in data sets where the content of the respective phases were approaching zero. At higher phase content the peak shapes are well defined, and there is very low correlation with background parameters. Further, the observed crystallite sizes are larger than the minimum constrained sizes. Selected data fits are shown in Fig. S6-S15.

Time (hrs.)	Temp. (°C)	R_{wp} (%)	Cu (wt%)	D_{Cu} (Å)	Scale	a_{Cu} (Å)	HKUST-1 (wt%)	$D_{HKUST-1}$ (Å)	Scale	$a_{HKUST-1}$ (Å)	O1 occ	Ow1 occ	Cu ₂ O (wt%)	D_{Cu_2O} (Å)	Scale	a_{Cu_2O} (Å)	Position (°)	Intensity
0.00	28	7	0.5	200	1.065E-03	3.650	97.9	6960	1.264E-05	26.300	0.888	0.289	1.6	100	1.793E-03	4.280	22.986	2.127E+01
0.17	28	7	0.5	200	9.549E-04	3.650	98.2	7037	1.283E-05	26.300	0.914	0.279	1.4	100	1.557E-03	4.280	22.988	2.152E+01
0.34	28	7	0.4	200	7.517E-04	3.650	97.9	7089	1.307E-05	26.300	0.961	0.244	1.8	100	2.078E-03	4.280	22.985	2.288E+01
0.54	48	7	0.0	200	9.716E-05	3.650	98.4	6866	1.354E-05	26.300	1.058	0.161	1.5	100	1.852E-03	4.280	22.972	2.325E+01
0.71	48	7	0.1	200	2.676E-04	3.650	98.4	6825	1.378E-05	26.300	1.078	0.070	1.4	100	1.723E-03	4.280	22.970	2.367E+01
0.95	50	7	0.1	200	1.245E-04	3.650	98.3	6598	1.413E-05	26.300	1.063	0.024	1.6	100	1.992E-03	4.280	22.965	2.437E+01
1.17	73	7	0.0	9986	9.407E-05	3.637	98.4	6709	1.441E-05	26.300	1.053	0.009	1.5	100	1.886E-03	4.280	22.946	2.467E+01
1.34	73	7	0.0	9998	1.016E-04	3.638	98.5	6769	1.458E-05	26.300	1.021	0.000	1.4	100	1.805E-03	4.280	22.944	2.597E+01
1.52	75	7	0.0	9998	1.051E-04	3.635	98.5	6838	1.478E-05	26.300	0.994	0.000	1.5	100	1.856E-03	4.280	22.941	2.604E+01
1.73	98	7	0.0	2409	1.175E-07	3.633	98.5	6390	1.514E-05	26.295	0.921	0	1.5	100	1.964E-03	4.280	22.917	2.622E+01
1.90	98	7	0.0	8620	2.858E-05	3.614	98.7	6321	1.535E-05	26.290	0.856	0	1.3	100	1.725E-03	4.280	22.913	2.613E+01
2.07	100	7	0.0	4400	8.576E-06	3.617	98.6	6277	1.572E-05	26.287	0.796	0	1.4	100	1.916E-03	4.280	22.915	2.631E+01
2.27	123	7	0.0	8602	2.758E-06	3.610	99.0	6136	1.606E-05	26.273	0.653	0	1.0	139	1.371E-03	4.277	22.895	2.740E+01
2.44	123	7	0.0	8602	6.576E-07	3.610	99.1	6071	1.631E-05	26.268	0.526	0	0.9	169	1.233E-03	4.278	22.891	2.752E+01
2.62	125	7	0.0	8601	1.364E-06	3.610	99.1	6087	1.648E-05	26.264	0.462	0	0.9	167	1.195E-03	4.278	22.894	2.734E+01

2.81	148	7	0.0	9310	2.804E-05	3.639	99.3	5927	1.667E-05	26.252	0.336	0	0.7	200	9.798E-04	4.275	22.869	2.741E+01
2.98	148	7	0.0	7166	9.215E-06	3.640	99.3	6005	1.683E-05	26.249	0.261	0	0.7	217	9.983E-04	4.276	22.866	2.770E+01
3.16	150	7	0.0	4400	1.175E-07	3.630	99.3	5957	1.706E-05	26.247	0.225	0	0.7	236	9.692E-04	4.276	22.864	2.777E+01
3.35	173	7	0.0	3032	1.957E-06	3.628	99.3	5788	1.718E-05	26.240	0.170	0	0.7	229	9.866E-04	4.275	22.839	2.748E+01
3.52	173	7	0.0	3013	1.175E-07	3.628	99.3	5900	1.709E-05	26.240	0.140	0	0.7	229	9.550E-04	4.271	22.837	2.627E+01
3.70	175	7	0.0	1788	1.175E-07	3.630	99.3	5887	1.721E-05	26.239	0.119	0	0.7	234	9.358E-04	4.273	22.839	2.770E+01
3.89	198	7	0.0	3010	2.130E-06	3.610	99.3	5721	1.728E-05	26.234	0.099	0	0.7	274	8.957E-04	4.272	22.802	2.606E+01
4.07	198	7	0.0	3470	1.175E-07	3.627	99.3	5724	1.723E-05	26.234	0.090	0	0.7	269	9.614E-04	4.272	22.810	2.574E+01
4.24	200	7	0.0	5922	1.175E-07	3.605	99.3	5790	1.727E-05	26.234	0.087	0	0.7	241	9.727E-04	4.273	22.808	2.597E+01
4.43	223	7	0.0	3470	1.175E-07	3.627	99.3	5716	1.727E-05	26.231	0.086	0	0.7	245	9.880E-04	4.271	22.771	2.351E+01
4.61	223	7	0.0	3568	1.175E-07	3.609	99.3	5738	1.719E-05	26.231	0.080	0	0.7	264	1.008E-03	4.271	22.780	1.938E+01
4.78	225	7	0.0	3089	2.117E-06	3.627	99.2	5704	1.721E-05	26.231	0.083	0	0.8	237	1.097E-03	4.272	22.769	1.767E+01
4.97	248	7	0.0	5941	1.943E-07	3.605	98.9	5757	1.709E-05	26.228	0.076	0	1.1	201	1.502E-03	4.271	22.756	1.156E+01
5.15	248	7	0.0	6743	2.381E-06	3.636	98.8	5764	1.709E-05	26.228	0.078	0	1.2	203	1.607E-03	4.270	22.754	8.682E+00
5.32	250	7	0.0	3472	6.709E-06	3.627	98.6	5832	1.701E-05	26.228	0.068	0	1.4	204	1.844E-03	4.270	22.743	6.374E+00
5.52	273	7	0.0	6743	2.217E-05	3.607	98.3	5639	1.702E-05	26.226	0.081	0	1.7	190	2.301E-03	4.270	22.700	4.479E+00
5.69	273	7	0.1	9999	1.426E-04	3.626	98.0	5670	1.691E-05	26.226	0.070	0	1.9	186	2.585E-03	4.270	22.700	2.703E+00
5.86	275	7	0.0	6781	7.269E-06	3.634	97.9	5555	1.686E-05	26.226	0.087	0	2.1	188	2.791E-03	4.269	22.701	1.940E+00
6.06	298	7	0.1	9997	3.196E-04	3.629	97.5	5094	1.619E-05	26.226	0.105	0	2.4	189	3.158E-03	4.268	23.100	3.200E-04
6.23	298	7	0.5	5697	8.148E-04	3.631	96.2	2336	1.147E-05	26.232	0.180	0	3.4	188	3.208E-03	4.268	22.703	3.200E-04
6.41	300	7	8.3	869	3.480E-03	3.635	70.5	800	1.867E-06	26.275	0.000	0	21.2	125	4.871E-03	4.268	23.100	3.200E-04
6.60	323	7	86.8	806	5.379E-02	3.636	3.1	800	1.347E-07	26.201	0.000	0	10.1	100	3.417E-03	4.276	22.852	3.200E-04
6.78	323	7	92.0	712	4.517E-02	3.634							8.0	100	2.140E-03	4.280	22.991	3.200E-04
6.95	325	7	93.4	693	4.468E-02	3.634							6.6	100	1.707E-03	4.280	23.100	3.200E-04
7.14	348	7	97.6	664	4.521E-02	3.636							2.4	100	6.024E-04	4.280	22.887	3.200E-04
7.32	348	7	99.8	658	4.598E-02	3.636							0.2	232	4.768E-05	4.220	22.986	3.200E-04

7.49	350	7	100.0	656	4.568E-02	3.636	0.0	218	8.650E-07	4.220	22.725	3.200E-04
7.69	373	7	100.0	647	4.631E-02	3.638	0.0	100	7.937E-07	4.280	23.053	3.200E-04
7.86	373	7	100.0	651	4.624E-02	3.638	0.0	460	7.630E-07	4.220	23.042	3.200E-04
8.03	375	7	100.0	651	4.624E-02	3.638	0.0	100	8.372E-07	4.280	22.966	3.200E-04
8.23	398	7	100.0	657	4.586E-02	3.639	0.0	100	7.308E-07	4.280	22.984	3.200E-04
8.40	398	7	100.0	653	4.574E-02	3.639	0.0	100	7.420E-07	4.280	22.805	3.200E-04
8.58	400	7	100.0	649	4.564E-02	3.639	0.0	100	7.029E-07	4.280	22.786	3.200E-04
8.76	423	7	100.0	650	4.488E-02	3.641	0.0	100	7.008E-07	4.280	22.986	3.200E-04
8.94	423	7	100.0	657	4.463E-02	3.641	0.0	100	6.645E-07	4.280	23.100	3.200E-04
9.11	425	7	100.0	654	4.466E-02	3.641	0.0	100	6.758E-07	4.280	22.739	3.200E-04
9.30	448	7	100.0	655	4.381E-02	3.643	0.0	100	3.274E-07	4.280	23.100	3.200E-04
9.47	448	7	100.0	658	4.364E-02	3.643	0.0	100	5.034E-07	4.280	23.100	3.200E-04
9.65	450	7	100.0	663	4.331E-02	3.643	0.0	100	3.445E-07	4.280	23.099	3.200E-04
9.83	473	7	100.0	665	4.276E-02	3.645	0.0	3426	1.277E-07	4.220	23.100	3.200E-04
10.00	473	7	100.0	659	4.297E-02	3.645	0.0	9991	1.420E-06	4.220	23.100	3.200E-04
10.18	475	7	100.0	666	4.262E-02	3.645	0.0	1417	1.277E-07	4.220	22.701	3.200E-04
10.36	498	7	100.0	666	4.210E-02	3.647	0.0	3392	1.277E-07	4.220	22.790	3.200E-04
10.54	498	7	100.0	664	4.169E-02	3.647	0.0	7164	4.146E-06	4.220	22.855	3.200E-04
10.71	500	7	99.9	663	4.175E-02	3.647	0.1	1770	1.762E-05	4.220	22.702	3.200E-04
10.89	500	7	99.9	664	4.165E-02	3.647	0.1	5660	1.237E-05	4.220	23.061	3.200E-04
11.06	500	7	100.0	668	4.152E-02	3.647	0.0	9980	1.277E-07	4.220	23.100	3.200E-04
11.23	500	7	100.0	659	4.197E-02	3.647	0.0	9985	1.552E-06	4.220	23.100	3.200E-04

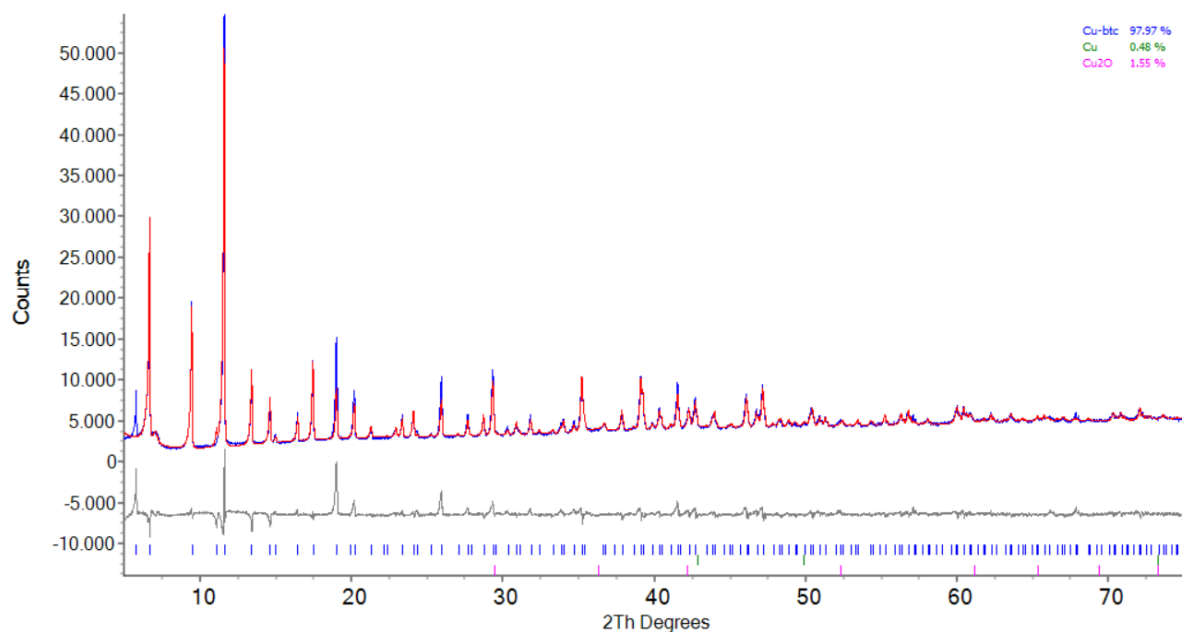


Fig. S6. Refinement of PXRD data ($t = 0.0$ h, $T = 28$ °C). Data (blue line), model (red line), and the difference between data and model (grey line). Refined composition (wt%): HKUST-1 (98.0 %), Cu_2O (1.6 %), Cu (0.5 %). The undescribed intensity of the (111) peak at 6° is ascribed to presence of water in the pores, which may influence the Bragg peak intensities (see for example reference 1 and 2).

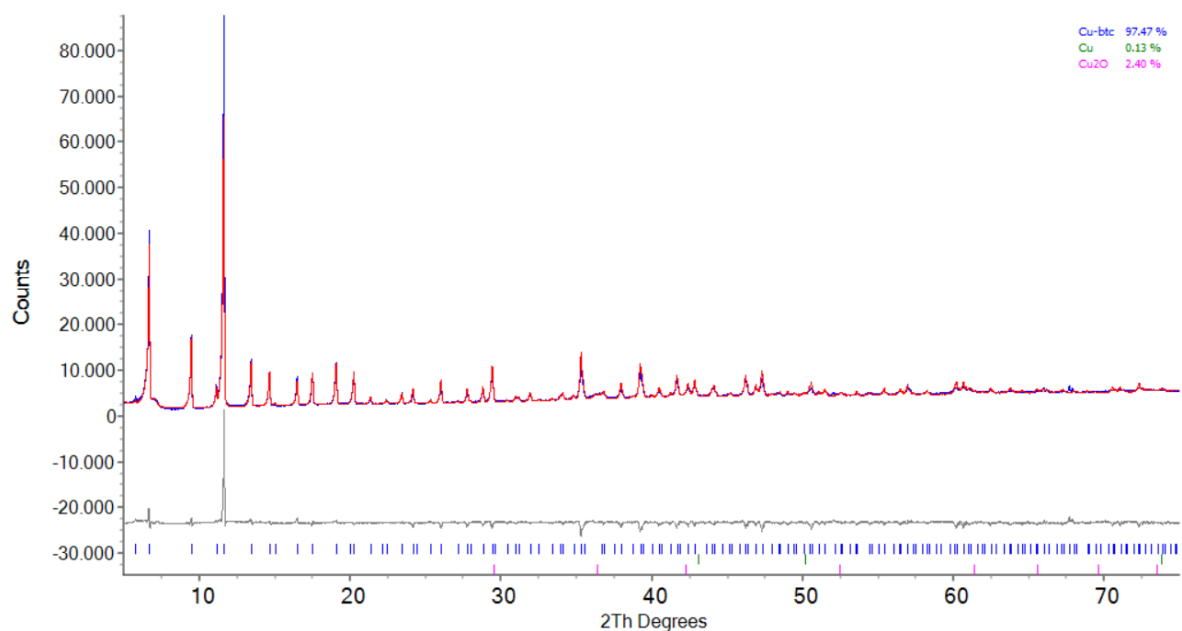


Fig. S7. Refinement of PXRD data ($t = 6.06$ h, $T = 298$ °C). Data (blue line), model (red line), and the difference between data and model (grey line). Refined composition (wt%): HKUST-1 (97.5 %), Cu_2O (2.4 %), Cu (0.1 %).

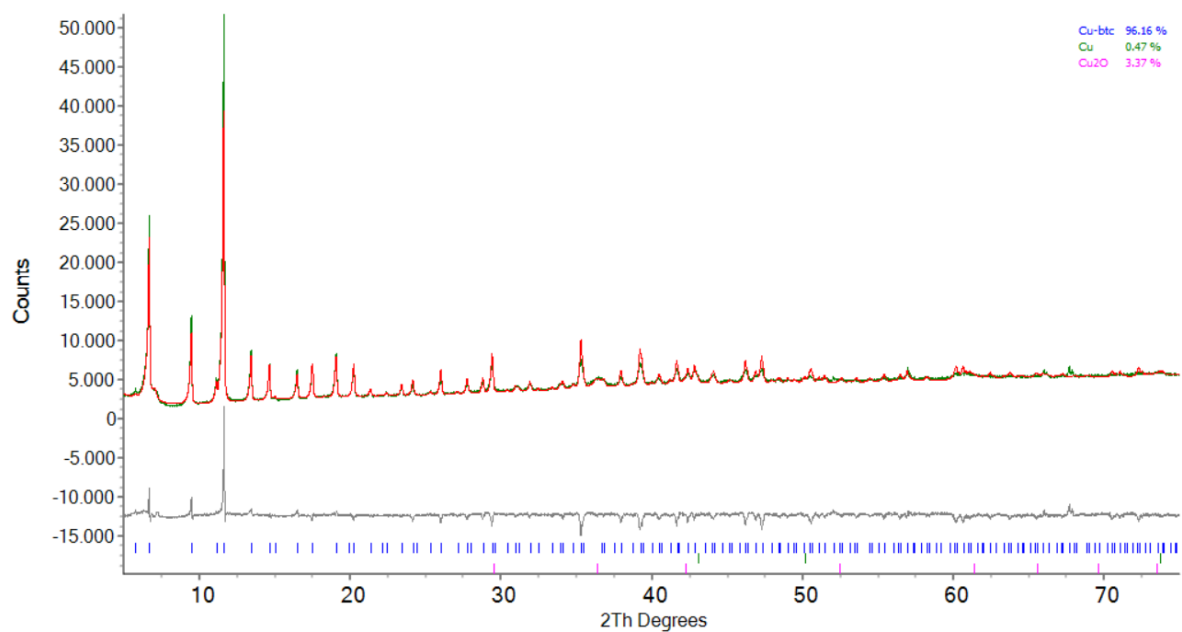


Fig. S8. Refinement of PXR D data ($t = 6.23$ h, $T = 298$ °C). Data (green line), model (red line), and the difference between data and model (grey line). Refined composition (wt%): HKUST-1 (96.2 %), Cu₂O (3.4 %), Cu (0.5 %).

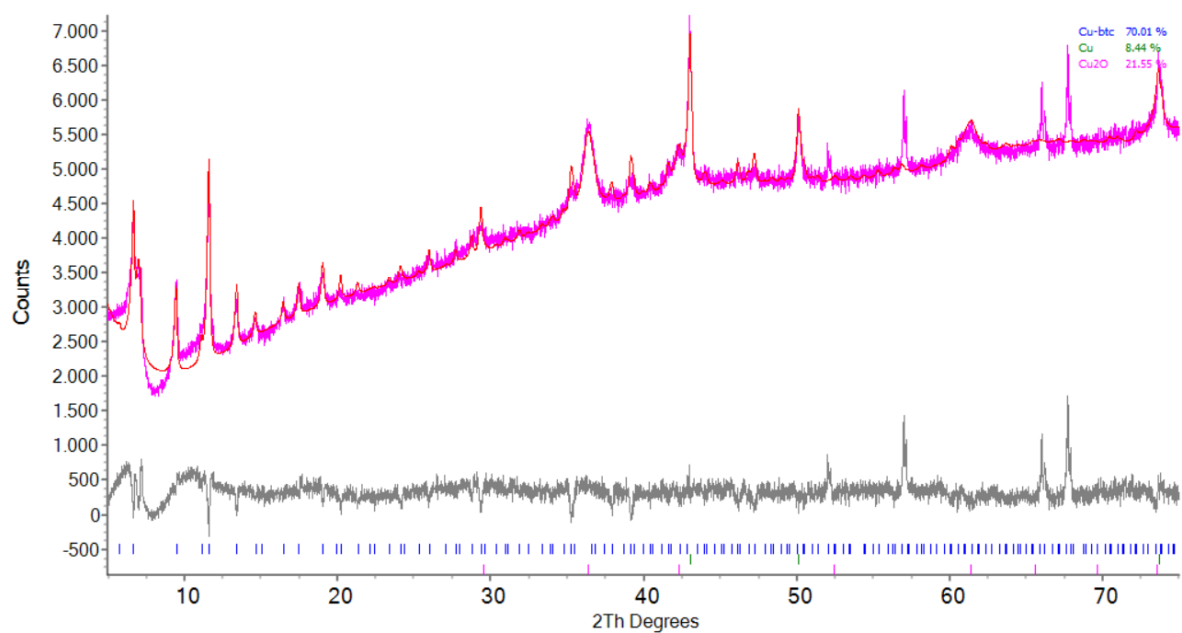


Fig. S9. Refinement of PXR D data ($t = 6.41$ h, $T = 300$ °C). Data (pink line), model (red line), and the difference between data and model (grey line). Refined composition (wt%): HKUST-1 (70.0 %), Cu₂O (21.6 %), Cu (8.4 %). Non-indexed peaks are from α -Al₂O₃ from the sample holder.

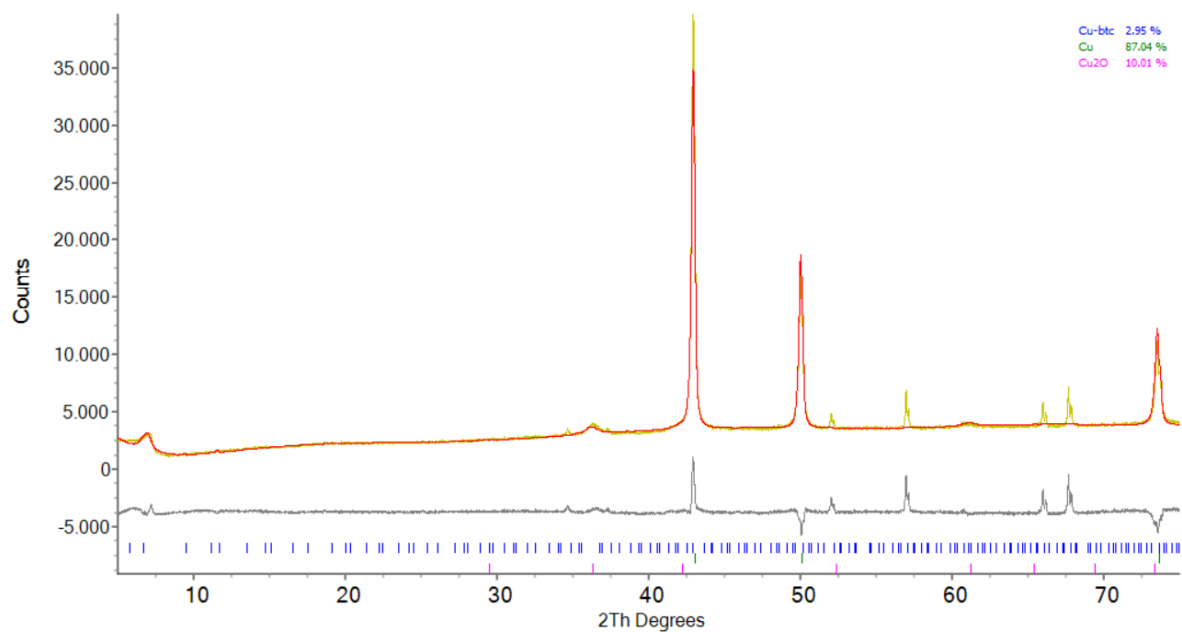


Fig. S10. Refinement of PXR D data ($t = 6.60$ h, $T = 323$ °C). Data (yellow line), model (red line), and the difference between data and model (grey line). Refined composition (wt%): HKUST-1 (3.0 %), Cu₂O (10.0 %), Cu (87.0 %). Non-indexed peaks are from α -Al₂O₃ from the sample holder.

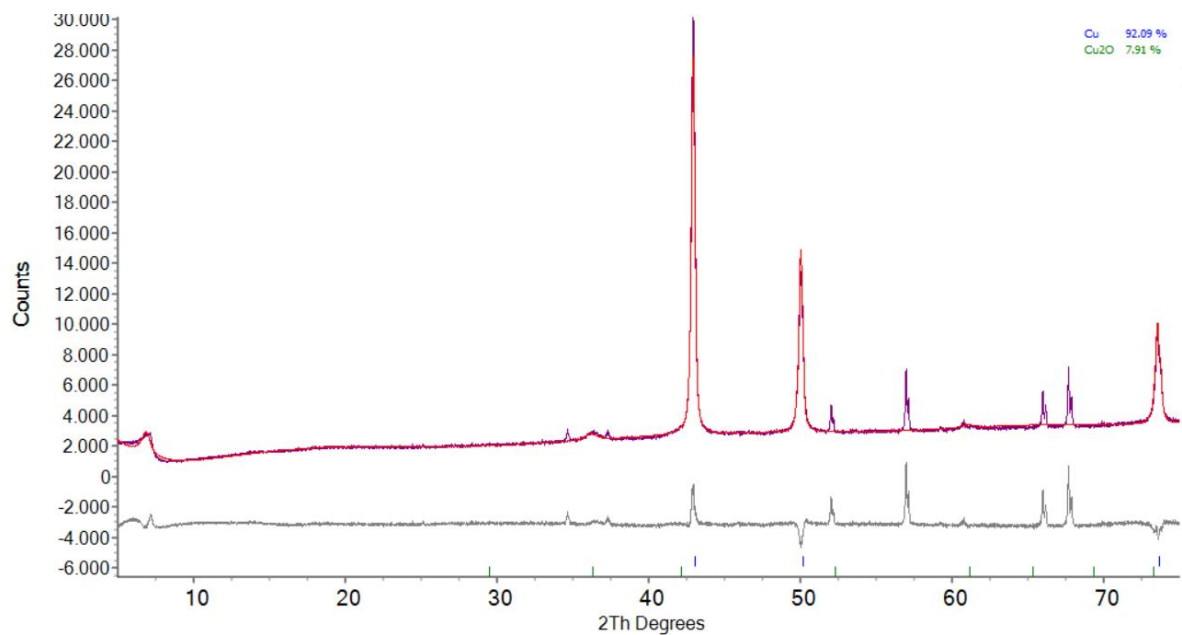


Fig. S11. Refinement of PXR D data ($t = 6.78$ h, $T = 323$ °C). Data (violet line), model (red line), and the difference between data and model (grey line). Refined composition (wt%): Cu₂O (7.9 %), Cu (92.1 %). Non-indexed peaks are from α -Al₂O₃ from the sample holder.

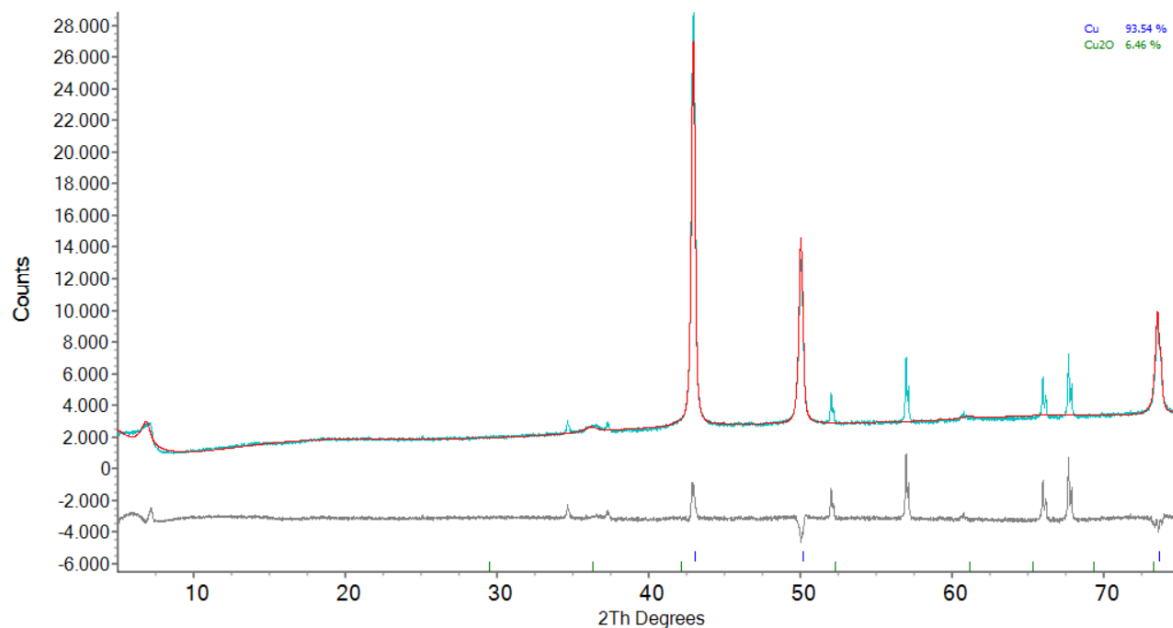


Fig. S12. Refinement of PXRD data ($t = 6.95$ h, $T = 325$ °C). Data (cyan line), model (red line), and the difference between data and model (grey line). Refined composition (wt%): Cu₂O (6.5 %), Cu (93.5 %). Non-indexed peaks are from α -Al₂O₃ from the sample holder.

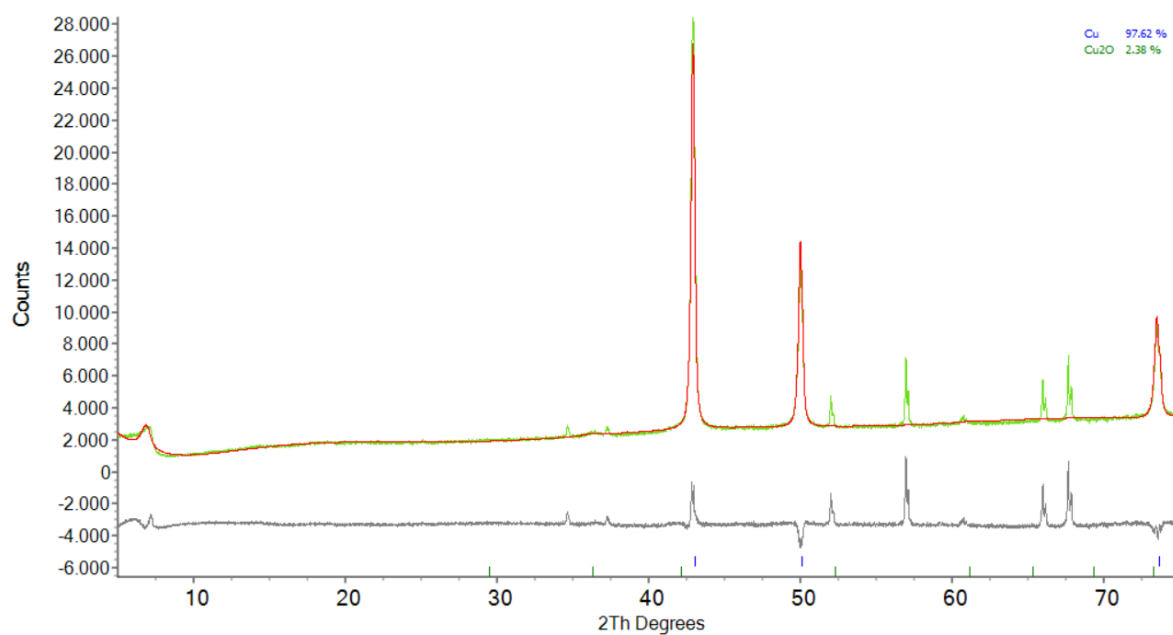


Fig. S13. Refinement of PXRD data ($t = 7.14$ h, $T = 348$ °C). Data (green line), model (red line), and the difference between data and model (grey line). Refined composition (wt%): Cu₂O (2.4 %), Cu (97.6 %). Non-indexed peaks are from α -Al₂O₃ from the sample holder.

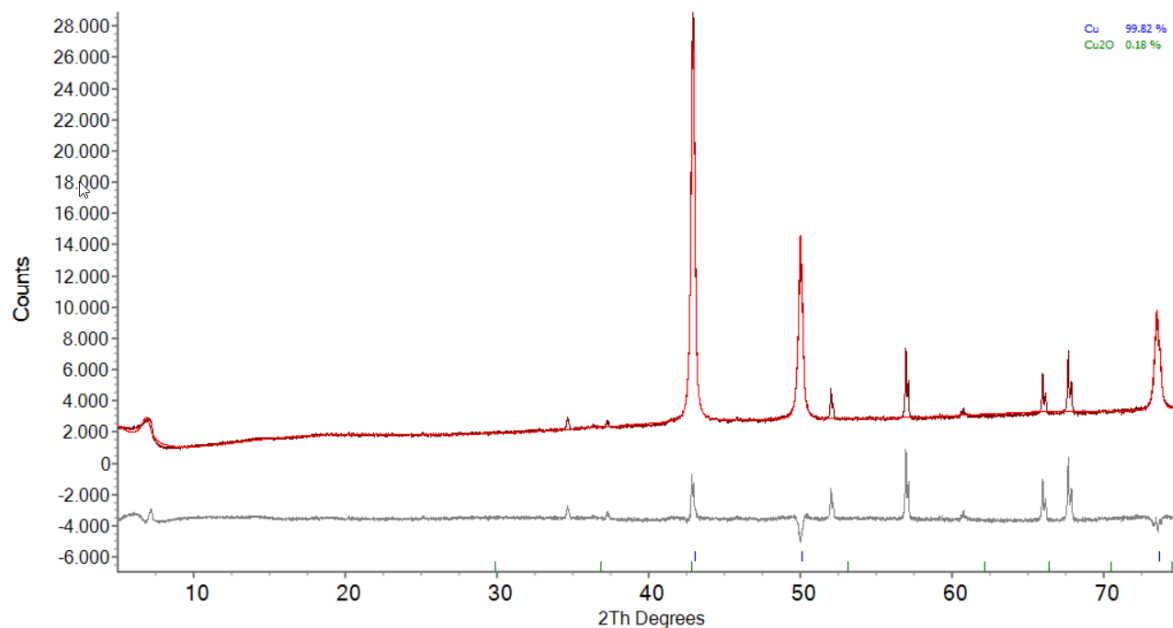


Fig. S14. Refinement of PXR D data ($t = 7.32$ h, $T = 348$ °C). Data (black line), model (red line), and the difference between data and model (grey line). Refined composition (wt%): Cu₂O (0.2 %), Cu (99.8 %). Non-indexed peaks are from α -Al₂O₃ from the sample holder.

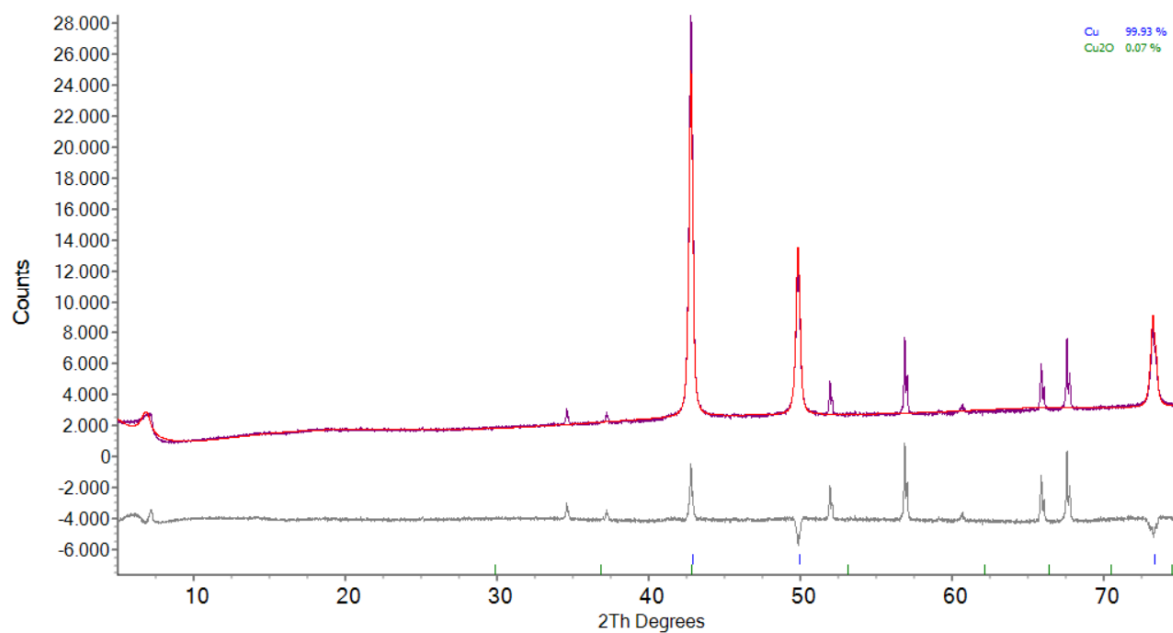


Fig. S15. Refinement of PXR D data ($t = 10.71$ h, $T = 500$ °C). Data (purple line), model (red line), and the difference between data and model (grey line). Refined composition (wt%): Cu₂O (0.1 %), Cu (99.9 %). Non-indexed peaks are from α -Al₂O₃ from the sample holder.

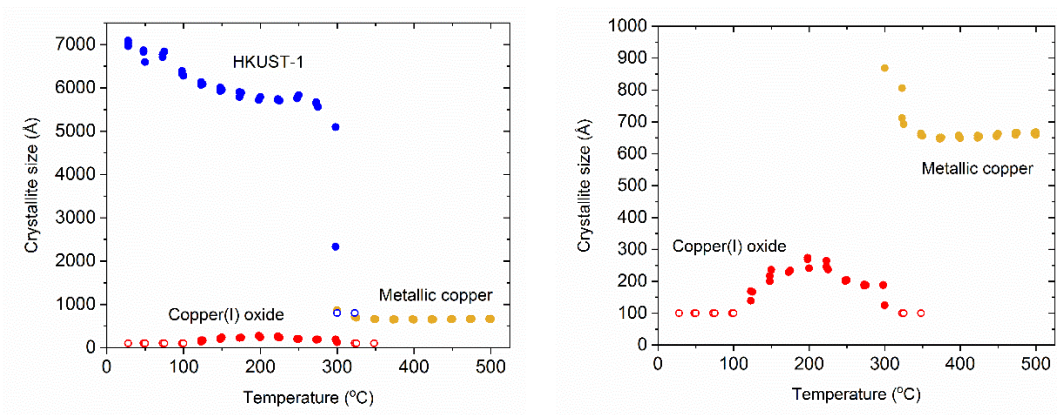


Fig. S16. Crystallite sizes obtained from Rietveld refinement. The figure to the left displays sizes of HKUST-1, Cu_2O and Cu, while the figure to the right only displays data for Cu_2O and Cu. Open symbols indicate the constrained minimum sizes during the refinements (see also Table S3). Only phases contributing more than 1 wt% at a given temperature have been included. The sizes of pristine HKUST-1 of approx. 6000-7000 Å should not be taken as actual crystal sizes, but rather it shows that the phase consists of large crystallites that scatter well. Copper(I) oxide formed from HKUST-1 appears to be slightly bigger than the already present impurity, while the final metallic copper particles interestingly does not appear to exhibit crystallite growth upon further heating, but has a constant size. This might be due to immobilization of the metal particles in the carbon matrix.

6. Total scattering and pair distribution function (PDF) analysis

6.1 Setup

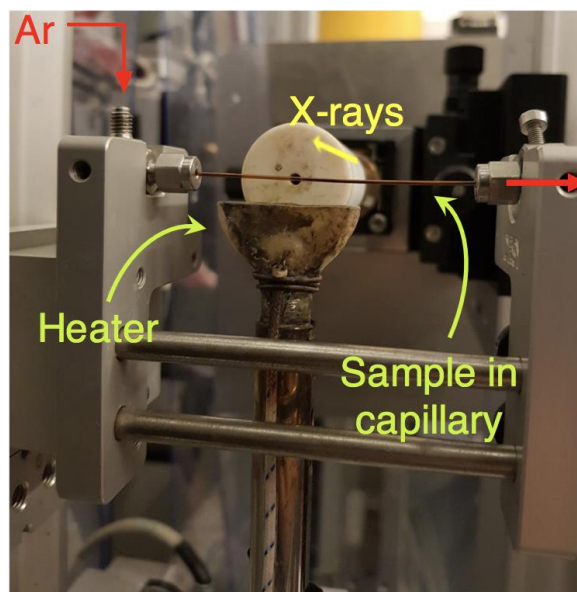


Fig. S17. Capillary setup for *in situ* total scattering experiments. HKUST-1 powder was packed in fused silica capillaries (inner diameter 0.7 mm, outer diameter 0.85 mm) for a high transmission of X-rays. The capillary was connected to the reactor using graphite ferrules and Swagelok fittings allowing an argon flow of 100 mL/min through the capillary. The sample containing capillary was heated by a jet of hot air from directly below. In the image, X-rays are coming towards the reader, and the Swagelok tubing for Ar is not connected. A thermocouple was inserted into the capillary before the experiments to determine the relation between the set temperature of the heater and real temperature at the sample position.

6.2 2 °C/min pyrolysis experiment

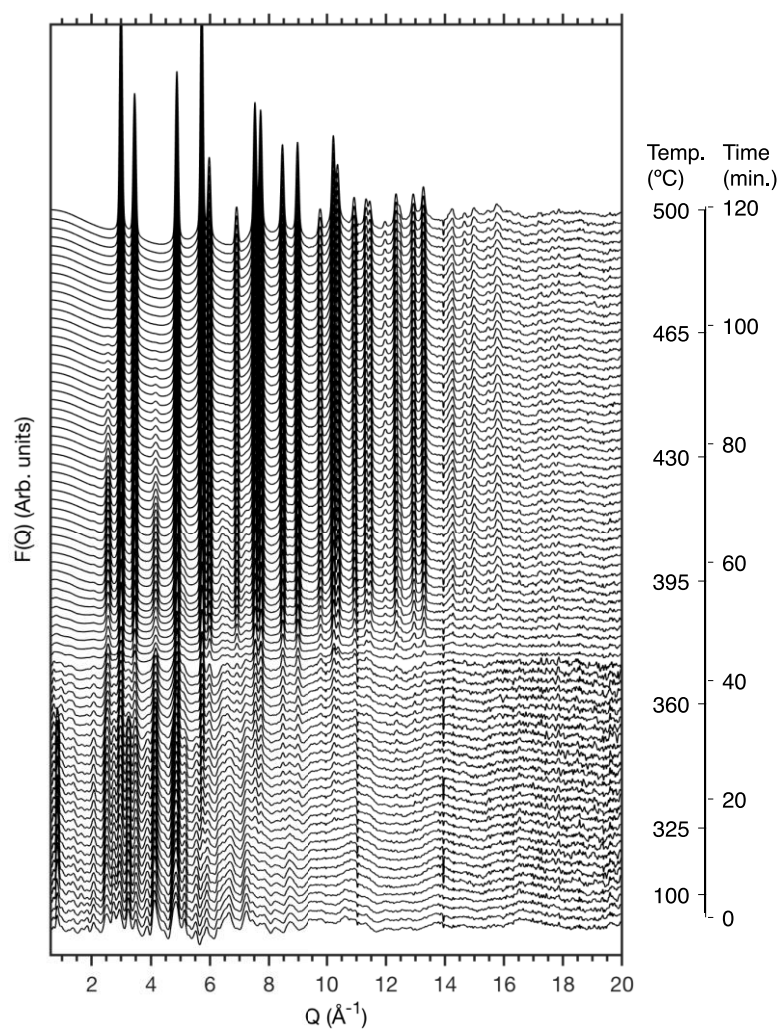


Fig. S18. Reduced total scattering structure function, $F(Q)$ of pyrolysis experiment using 2 °C/min heating ramp. Each $F(Q)$ corresponds to a data collection time of 1.5 minutes. A combined temperature/time axis is shown in the right of the figure.

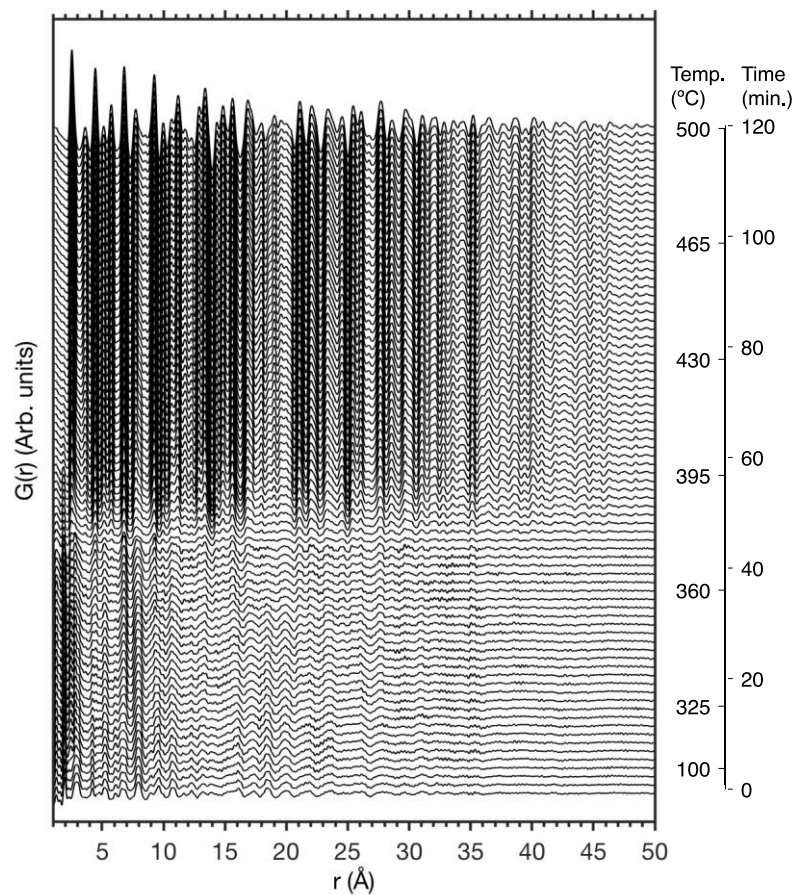


Fig. S19. Pair distribution functions, $G(r)$ of pyrolysis experiment using $2\text{ }^{\circ}\text{C}/\text{min}$ heating ramp. Each PDF corresponds to a data collection of 1.5 minutes. A combined temperature/time axis is shown in the right of the figure.

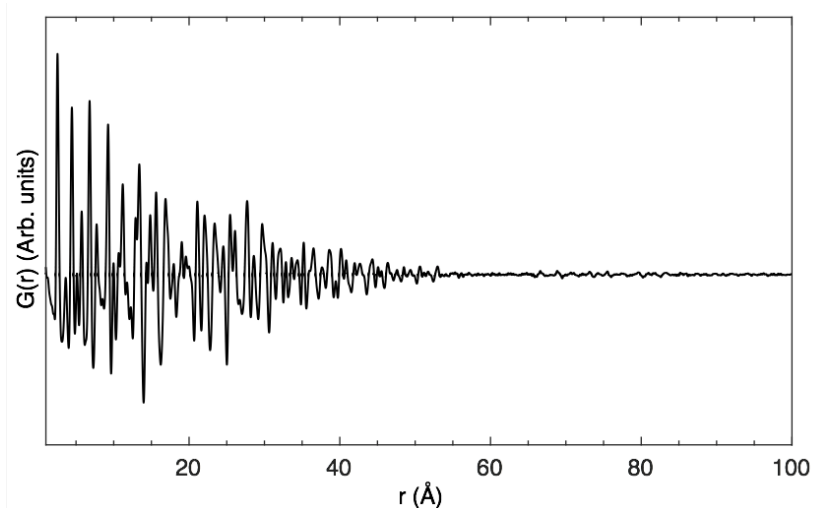


Fig. S20. Pair distribution function of the end point of the $2\text{ }^{\circ}\text{C}/\text{min}$ *in situ* pyrolysis experiment. The ordered structure of the metallic copper is seen by the PDF extending far in real space.

Table S4. Refinement of 2 °C/min PDFs in the range of 1-40 Å. Each PDF corresponds to a data collection time of 5 minutes. Reported are the temperature in degrees Celsius, R_w in percentage, the delta2 parameter, the phase fractions in weight percentage, the scale factor, the cubic unit cell parameter in Angstrom, and finally one isotropic atomic displacement parameter to describe all copper atoms (U_{Cu}) and one to describe all carbon and oxygen atoms (U_{org}). HKUST-1 was excluded from refinements above 367 °C due to unphysical cell parameters caused by the low content in the sample.

Temp. (°C)	R_w (%)	$\delta 2$	HKUST-1 (wt%)	scale	$a_{HKUST-1}$ (Å)	Cu ₂ O (wt%)	scale	a_{Cu_2O} (Å)	Cu (wt%)	scale	a_{Cu} (Å)	U_{Cu} (Å ²)	U_{org} (Å ²)
80	49.9	3.75	91.0	8.96E-02	26.305	9.0	2.378E-02	4.262				0.01922	0.022678
188	45.0	3.69	92.5	1.32E-01	26.240	7.5	2.888E-02	4.263				0.02242	0.045324
284	44.9	3.61	91.6	1.21E-01	26.223	8.4	3.013E-02	4.262				0.02446	0.041089
327	43.2	3.60	88.5	1.16E-01	26.221	8.9	3.165E-02	4.265	2.6	1.198E-02	3.629	0.0255	0.039691
333	43.2	3.58	87.3	1.13E-01	26.216	9.1	3.184E-02	4.265	3.6	1.662E-02	3.630	0.02513	0.039361
342	42.1	3.59	86.6	1.12E-01	26.213	8.9	3.145E-02	4.265	4.5	2.055E-02	3.631	0.02457	0.040807
351	45.3	3.54	82.1	8.46E-02	26.222	11.0	3.068E-02	4.262	6.9	2.524E-02	3.631	0.02401	0.034101
359	49.7	3.72	66.5	3.74E-02	26.228	19.3	2.951E-02	4.260	14.2	2.836E-02	3.632	0.02428	0.039826
367	47.2	3.40	66.9	4.00E-02	26.248	16.7	2.703E-02	4.259	16.4	3.473E-02	3.632	0.0209	0.032691
376	26.5	3.42				25.2	2.439E-02	4.269	74.8	9.430E-02	3.633	0.01549	0.021992
385	17.4	2.86				20.9	1.539E-02	4.266	79.1	7.582E-02	3.633	0.0148	0.046304
393	15.1	3.03				19.4	2.194E-02	4.267	80.6	1.189E-01	3.633	0.01479	0.06073
402	13.8	3.09				17.7	2.491E-02	4.268	82.3	1.514E-01	3.633	0.01494	0.068181
410	12.7	3.10				15.3	2.293E-02	4.269	84.7	1.655E-01	3.634	0.0151	0.074235
419	11.5	3.18				11.1	1.745E-02	4.271	88.9	1.817E-01	3.634	0.01532	0.088781
428	10.9	3.22				7.6	1.237E-02	4.274	92.4	1.972E-01	3.635	0.01561	0.103617
436	10.7	3.26				5.3	8.874E-03	4.279	94.7	2.083E-01	3.635	0.01587	0.035375
445	10.5	3.28				3.5	6.076E-03	4.289	96.5	2.169E-01	3.636	0.01617	0.01
453	10.4	3.30				2.5	4.437E-03	4.309	97.5	2.246E-01	3.636	0.01643	0.060446
462	10.3	3.30				1.7	3.038E-03	4.336	98.3	2.332E-01	3.637	0.01667	0.071847
471	10.3	3.30							100.0	2.392E-01	3.637	0.01687	
479	10.2	3.27							100.0	2.404E-01	3.638	0.01704	
488	10.2	3.29							100.0	2.407E-01	3.638	0.01728	
496	10.1	3.30							100.0	2.417E-01	3.639	0.01752	

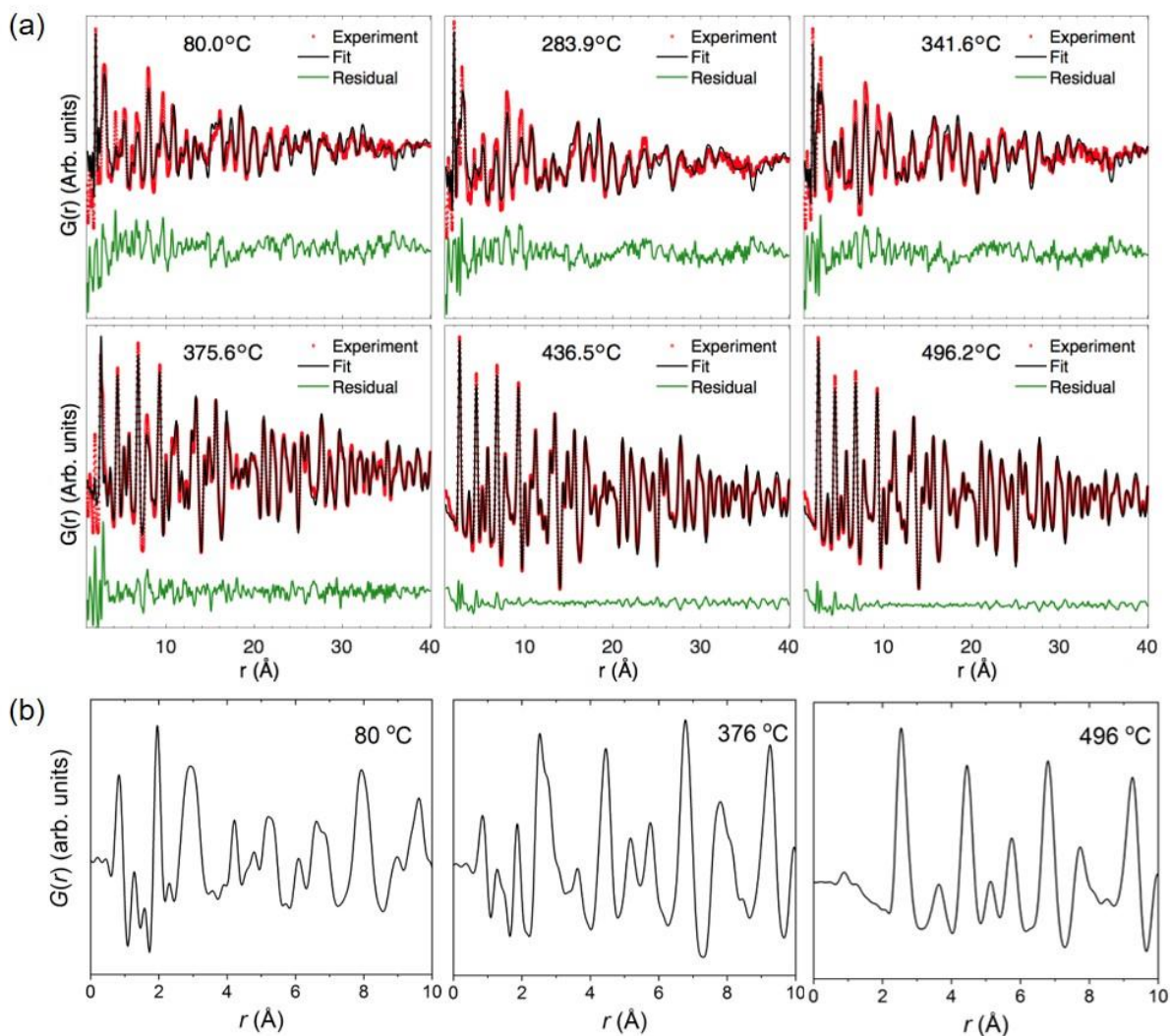


Fig. S21. (a) Selected fits from multiphase PDF refinement from data series collected with a heating ramp of 2 °C/min over $r = 1\text{-}40$ Å. Data points are shown as red circles, the model as a black line, and the difference between data and model is shown as a green line. HKUST-1 (hydrated or dehydrated), copper(I) oxide, and metallic copper are used as the phases to describe the data. Other common copper compounds (e.g. copper(II) oxide) have also been tested as additional phases in the refinements but never improved the fits. While the fits after the decomposition of HKUST-1 are very good, the fits of the pristine MOF are less so. The fits do however clearly encompass the features in the experimental data, the problem lies primarily in describing the relative intensities of the peaks, which might be due to an imperfect crystalline material. (b) Three of the data sets have been plotted in the range 1-10 Å. Unphysical artefacts below 1 Å are present, but decrease in relative intensity with the formation of metallic copper.

Table S5. Refinement of 2 °C/min PDFs in the range 1-15 Å (short range). Each PDF corresponds to a data collection time of 5 minutes. Reported are the temperature in degrees Celsius, R_w in percentage, the delta2 parameter, the phase fractions in weight percentage, the scale factor, the cubic unit cell parameter in Angstrom, and finally one isotropic atomic displacement parameter to describe all copper atoms (U_{Cu}) and one to describe all carbon and oxygen atoms (U_{org}).

Temp. (°C)	R_w (%)	δ_2	HKUST-1 (wt%)	scale	$a_{HKUST-1}$ (Å)	Cu ₂ O (wt%)	scale	a_{Cu_2O} (Å)	Cu (wt%)	scale	a_{Cu} (Å)	U_{Cu} (Å ²)	U_{org} (Å ²)
80	43.1	3.695	88.4	9.60E-02	26.303	11.6	3.38E-02	4.248	0.0			0.0210	0.01908
188	38.9	3.598	89.0	1.23E-01	26.242	11.0	4.10E-02	4.252	0.0			0.02413	0.03473
284	39.2	3.557	89.6	1.33E-01	26.167	10.4	4.18E-02	4.257	0.0			0.02662	0.04183
327	36.9	3.545	86.5	1.28E-01	26.175	10.9	4.38E-02	4.258	2.6	1.35E-02	3.656	0.02786	0.0377
333	37.0	3.527	85.6	1.26E-01	26.170	10.9	4.34E-02	4.259	3.5	1.82E-02	3.649	0.02731	0.0352
342	36.1	3.585	84.6	1.23E-01	26.167	11.0	4.34E-02	4.260	4.4	2.26E-02	3.645	0.02705	0.04049
351	38.1	3.527	81.4	1.01E-01	26.148	12.4	4.19E-02	4.261	6.1	2.69E-02	3.641	0.02639	0.03272
359	43.1	3.721	62.8	4.20E-02	26.229	23.3	4.24E-02	4.254	13.8	3.28E-02	3.645	0.02747	0.017
367	40.8	3.407	67.9	5.16E-02	26.037	18.1	3.74E-02	4.264	14.0	3.77E-02	3.638	0.02325	0.01333
376	27.5	2.590	0.0			29.8	3.23E-02	4.258	70.2	9.92E-02	3.635	0.01543	0.00206
385	17.8	2.580	0.0			25.0	2.00E-02	4.260	75.0	7.79E-02	3.634	0.01465	0.00678
393	14.4	2.660	0.0			22.8	2.80E-02	4.262	77.2	1.23E-01	3.634	0.01452	0.01125
402	12.8	2.712	0.0			20.6	3.14E-02	4.263	79.4	1.57E-01	3.634	0.01465	0.01399
410	11.8	2.752	0.0			17.9	2.88E-02	4.264	82.1	1.72E-01	3.634	0.01482	0.01707
419	10.5	2.904	0.0			13.2	2.21E-02	4.266	86.8	1.89E-01	3.635	0.01505	0.0289
428	9.8	2.945	0.0			9.1	1.59E-02	4.261	90.9	2.06E-01	3.635	0.01537	0.0258
436	9.5	2.982	0.0			6.5	1.16E-02	4.262	93.5	2.17E-01	3.636	0.01562	0.0328
445	9.4	3.009	0.0			4.6	8.32E-03	4.262	95.4	2.26E-01	3.636	0.0159	0.03888
453	9.4	3.025	0.0			3.0	5.56E-03	4.263	97.0	2.34E-01	3.637	0.01614	0.04031
462	9.5	3.030	0.0			1.6	3.05E-03	4.264	98.4	2.43E-01	3.637	0.0164	0.04694
471	9.5	2.991	0.0			0.0			100.0	2.50E-01	3.638	0.01662	
479	9.5	2.995	0.0			0.0			100.0	2.51E-01	3.638	0.01681	
488	9.6	2.993	0.0			0.0			100.0	2.51E-01	3.639	0.01703	
496	9.6	2.999	0.0			0.0			100.0	2.52E-01	3.639	0.01726	

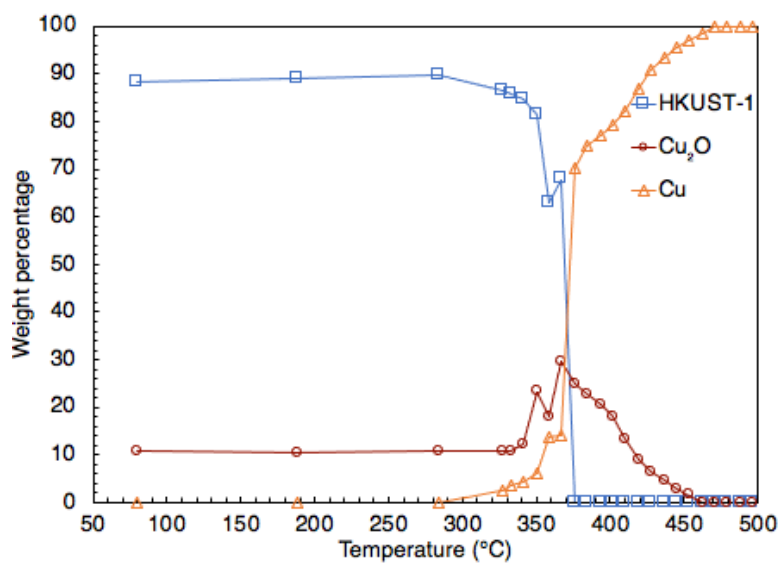


Fig. S22. Phase evolution from short range (1-15 Å) PDF refinement of 2 °C/min data.

6.3 5 °C/min pyrolysis experiment

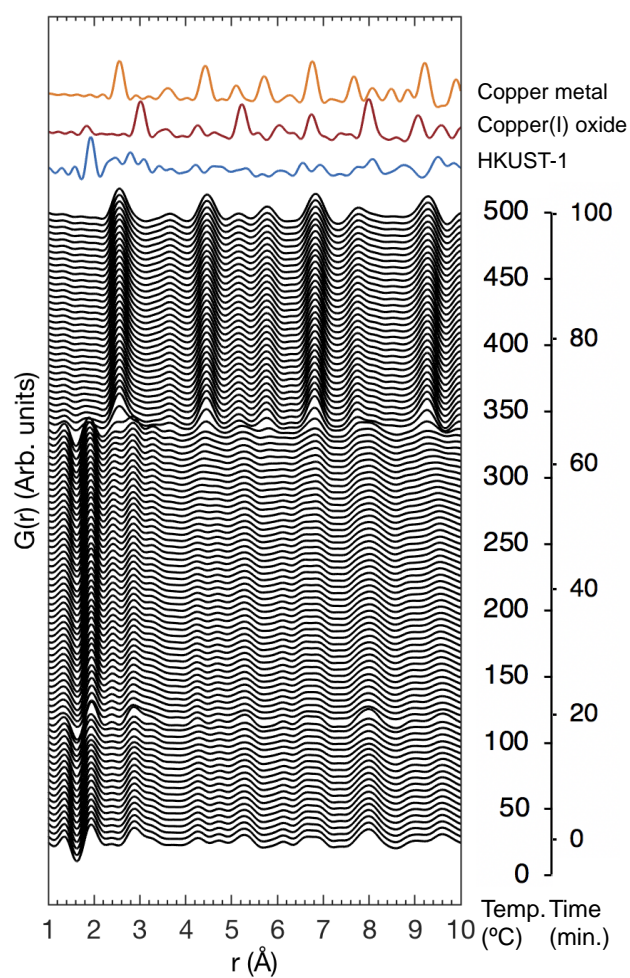


Fig. S23. *In situ* PDF data of HKUST-1 pyrolysis with calculated PDFs of metallic copper (yellow), copper(I) oxide (red), and dehydrated HKUST-1 (blue). A combined temperature/time axis is shown in the right of the figure. The PDFs shown are summed over 1 minute of data collection.

Table S6. Refinement of 5 °C/min PDFs in the range of 1-40 Å. Selected PDFs each corresponding to a data collection time of 1 minute are used. Reported are the temperature in degrees Celsius, R_w in percentage, the delta2 parameter, the phase fractions in weight percentage, the scale factor, the cubic unit cell parameter in Angstrom, and finally one isotropic atomic displacement parameter to describe all copper atoms (U_{Cu}) and one to describe all carbon and oxygen atoms (U_{org}).

Temp. (°C)	R_w (wt%)	$\delta 2$	HKUST-1 (wt%)	scale	$a_{HKUST-1}$ (Å)	Cu ₂ O (wt%)	scale	a_{Cu_2O} (Å)	Cu (wt%)	scale	a_{Cu} (Å)	U_{Cu} (Å ²)	U_{org} (Å ²)
25	48.8	3.264	88.2	2.08E-01	26.317	11.8	7.50E-02	4.263				0.02651	0.01286
100	51.1	3.211	89.9	1.72E-01	26.338	10.1	5.20E-02	4.263				0.02951	0.00785
200	41.9	3.408	91.4	2.22E-01	26.357	8.6	5.70E-02	4.269				0.03463	0.02474
300	45.0	3.433	92.0	2.50E-01	26.191	8.0	5.93E-02	4.280				0.03841	0.03122
325	46.2	3.409	86.8	2.12E-01	26.304	10.3	6.83E-02	4.270	2.9	2.47E-02	3.644	0.04579	0.01912
350	45.7	3.393	75.8	1.40E-01	25.937	16.6	8.29E-02	4.284	7.6	4.95E-02	3.646	0.04426	0.03146
355	16.3	3.393	32.3	6.89E-02	26.773	20.2	8.42E-02	4.265	47.4	2.41E-01	3.644	0.04426	0.03146
360	10.1	2.702	17.7	4.12E-02	27.015	13.6	5.04E-02	4.271	68.7	3.29E-01	3.644	0.03266	0.03146
365	8.6	2.683	18.6	3.22E-02	27.231	12.8	5.19E-02	4.276	68.6	3.38E-01	3.644	0.03153	0.03146
370	8.4	2.596	9.9	2.94E-02	27.303	16.6	6.01E-02	4.277	73.4	3.35E-01	3.645	0.03211	0.03146
375	8.4	2.543				16.8	5.76E-02	4.277	83.2	3.44E-01	3.646	0.03221	0.01000
400	7.7	2.596				12.2	4.02E-02	4.277	87.8	3.66E-01	3.647	0.03045	0.01000
425	7.6	2.688				2.6	5.81E-03	4.288	97.4	3.94E-01	3.650	0.01572	0.01000
450	7.6	2.693							100.0	4.06E-01	3.651	0.01750	
475	7.7	2.712							100.0	4.01E-01	3.653	0.01832	
500	7.9	2.710							100.0	3.96E-01	3.655	0.01910	

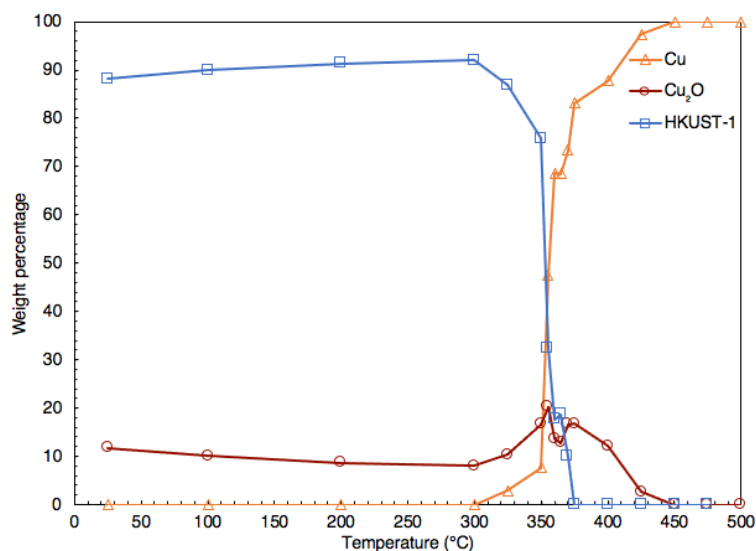


Fig. S24. Phase evolution from PDF (1-40 Å) refinement of 5 °C/min data.

6.4 Rapid heating pyrolysis experiment

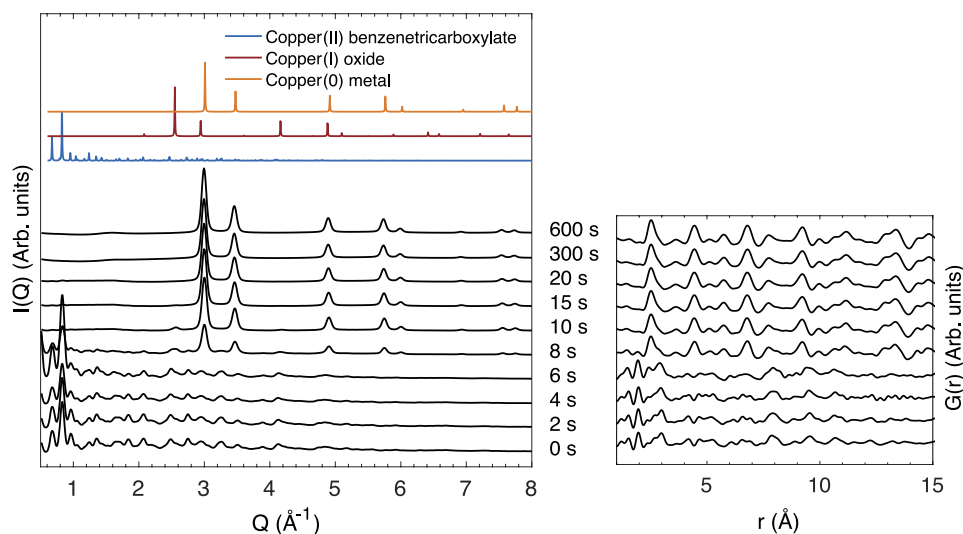


Fig. S25. Total scattering (left) and PDF (right) of rapid heating pyrolysis, i.e. reaching the target temperature of 500 °C within 8-10 s. Experimental data are shown in black, while calculated patterns are shown in blue (HKUST-1), red (Cu₂O) and yellow (metallic copper).

Table S7. Refinement of rapid heating PDFs in the range 1-40 Å. The initial six PDFs correspond to a data collection time of 2 seconds, the following two PDFs 5 seconds, and the last two PDFs correspond to a collection time of 1 minute. Reported are time in seconds, R_w in percentage, the delta2 parameter, the phase fractions in weight percentage, the scale factor, the cubic unit cell parameter in Angstrom, and finally one isotropic atomic displacement parameter to describe all copper atoms (U_{Cu}) and one to describe all carbon and oxygen atoms (U_{org}).

Time (sec)	R_w (wt%)	δ_2	HKUST-1 (wt%)	scale	$a_{HKUST-1}$ (Å)	Cu ₂ O (wt%)	scale	a_{Cu_2O} (Å)	Cu (wt%)	scale	a_{Cu} (Å)	U_{Cu} (Å ²)	U_{org} (Å ²)
0	50.9	3.731	92.7	7.35E-02	26.234	7.3	1.55E-02	4.212				0.01352	0.010014
2	55.0	3.734	90.6	6.40E-02	26.293	9.4	1.80E-02	4.224				0.01628	0.01149
4	59.5	3.637	91.3	6.23E-02	26.338	8.7	1.61E-02	4.221				0.01541	0.011528
6	47.9	3.072	95.8	1.23E-01	26.197	4.2	1.48E-02	4.213				0.01892	0.027534
8	18.2	3.077	54.0	5.34E-02	26.237	5.5	1.46E-02	4.229	40.5	1.42E-01	3.626	0.01843	0.017332
10	12.7	2.985	19.8	2.11E-02	26.684				80.2	3.02E-01	3.626	0.01899	0.008843
15	12.4	3.085	13.3	1.39E-02	26.202				86.7	3.21E-01	3.627	0.01995	0.002968
20	12.3	3.043							100.0	3.39E-01	3.631	0.02097	
300	11.1	3.031							100.0	5.01E-01	3.635	0.02253	
600	11.5	3.087							100.0	4.15E-01	3.634	0.02243	

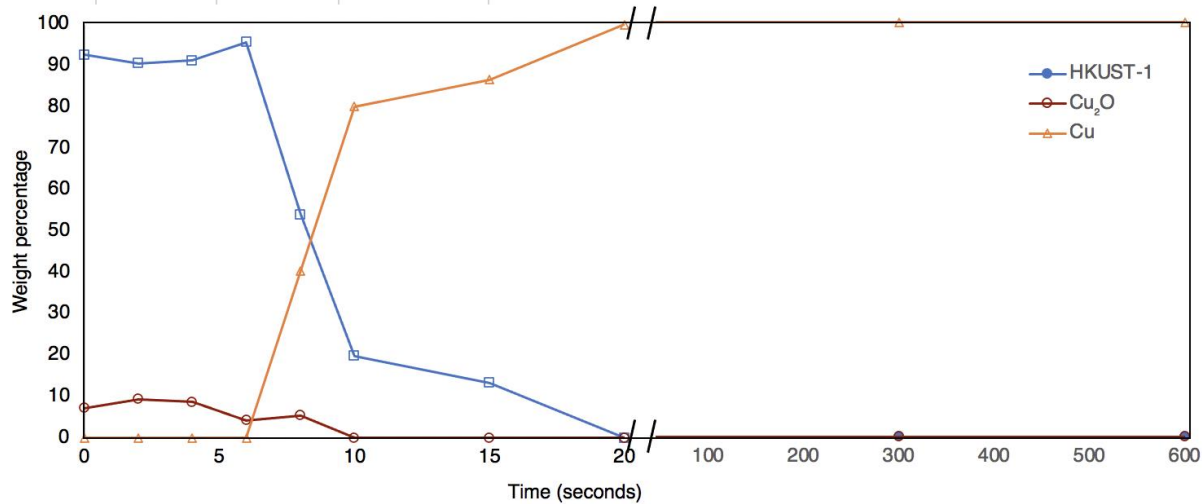


Fig. S26. Phase evolution from PDF (1-40 Å) refinement of rapid heating.

7. PXRD and PDF scale factors

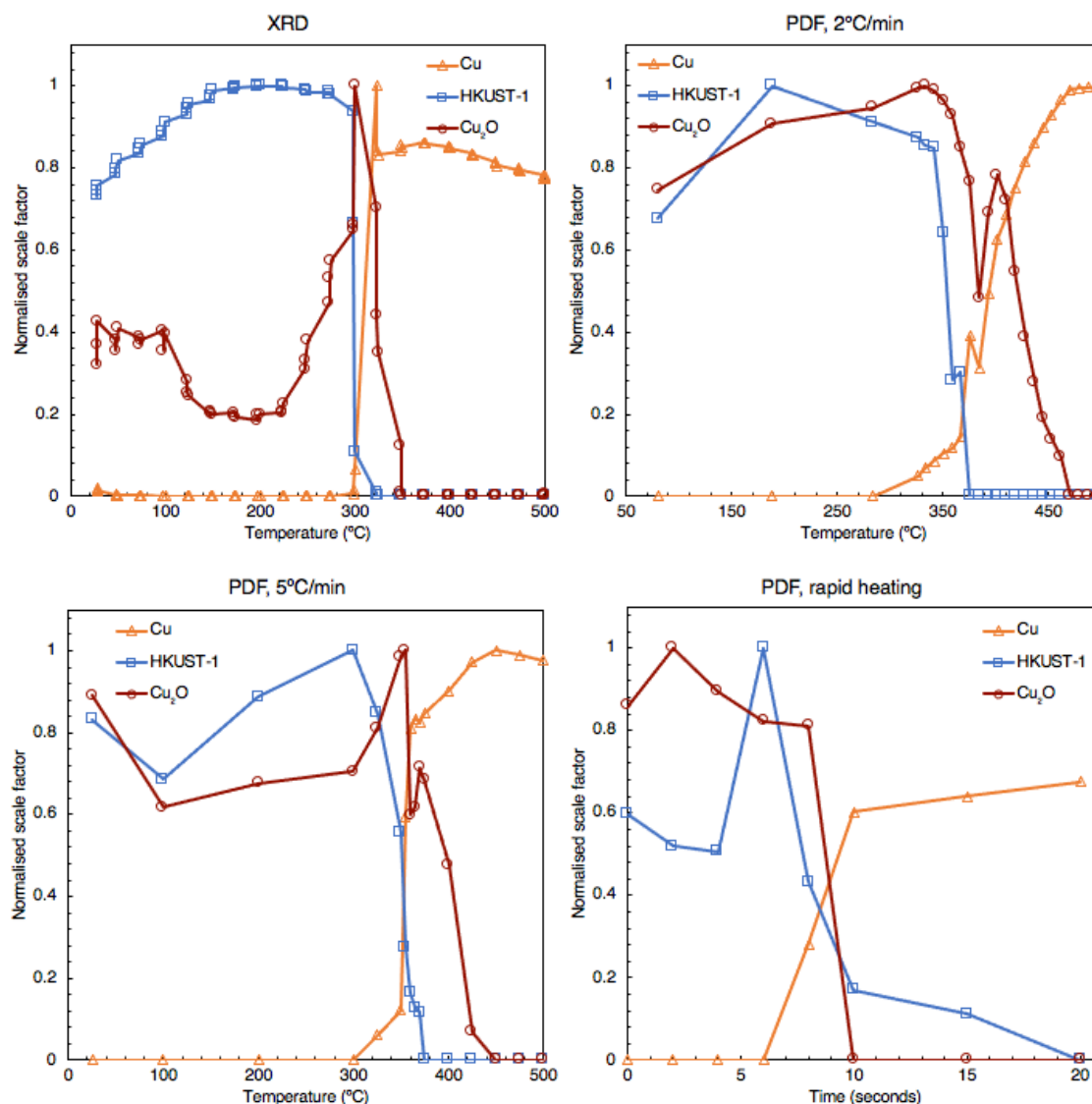


Fig. S27. Normalised scale factors for PXRD and PDF Rietveld refinements. For phase evolution investigations it is important to not only analyse the phase fractions in terms of wt% or mole%, since these are inherently correlated, but a look at the scale factors is necessary as these are independent for each phase. Especially in experiments like these where the mass changes due to the removal of gaseous organic pyrolysis products (and due to the oxide impurity in the starting mixture), we cannot be sure that the changes in wt% are necessarily depicting the real changes in phase amounts. Clearly the Cu₂O scale factor for the *in situ* PXRD analysis grows upon HKUST-1 decomposition (top left). Initially, the 2 and 5 °C/min PDF experiments (top right and bottom left) show a large scale factor for the oxide due to the higher amount of the impurity compared to PXRD. Specifically, the heaviest particles were removed gravimetrically from the powder prior to the PXRD experiment to reduce texturing. This might have led to a smaller oxide impurity in the PXRD sample as compared to the PDF samples, as Cu₂O has a higher density compared to HKUST-1. Moreover, PXRD, in contrast to PDF, only detects the crystalline Cu₂O content. The change to the oxide scale factor above the decomposition point of HKUST-1 stems from a combination of (i) the reduction of the oxide phase to metallic copper and (ii) the formation of new oxide from HKUST-1 (and partly the reduction of this when formed). Above 385 °C and 360 °C for the 2 °C/min and 5 °C/min experiments, respectively, the metal scale factors increase at a fast rate. No indications of additional oxide formation is seen in the rapid heating experiment (bottom right).

References

1. P. Lamagni, B. L. Pedersen, A. Godiksen, S. Mossin, X.-M. Hu, S. U. Pedersen, K. Daasbjerg and N. Lock, *RSC Advances*, 2018, **8**, 13921-13932.
2. A. Kathuria, M. G. Abiad and R. Auras, *Polymer International*, 2013, **62**, 1144-1151.